Multiobjective Optimization by Decomposition with Pareto-adaptive Weight Vectors

Siwei Jiang[1,2], *Student Member, IEEE*, Zhihua Cai[2], Jie Zhang[1], Yew-Soon Ong[1]
School of Computer Engineering, Nanyang Technology University, Singapore[1]
School of Computer Science, China University of Geosciences, Wuhan, China[2]

***Abstract*—MOEA/D is a recently proposed methodology of Multiobjective Evolution Algorithms that decomposes multiobjective problems into a number of scalar subproblems and optimizes them simultaneously. However, classical MOEA/D uses same weight vectors for different shapes of Pareto front. We propose a novel method called Pareto-adaptive weight vectors ($pa\lambda$) to automatically adjust the weight vectors by the geometrical characteristics of Pareto front. Evaluation on different multiobjective problems confirms that the new algorithm obtains higher hypervolume, better convergence and more evenly distributed solutions than classical MOEA/D and NSGA-II.**

I. Introduction

Many real-world problems can be described as Multiobjective problems (MOPs). MOPs always have several conflict objectives, and it is difficult to simultaneously optimize all the objectives. The tradeoff point is a Pareto-optimal solution, the set of Pareto-optimal solutions is called the *Pareto Set* (PS), and the set of all Pareto-optimal objective vectors is the *Pareto front* (PF). Multiobjective Evolutionary Algorithms (MOEAs) are demonstrated to be suitable for solving various complex MOPs [1].

Currently, most MOEAs are Pareto dominance-based algorithms such as NSGA-II [2], SPEA2 [3], SMPSO [4]. These algorithms use the Pareto dominance relation together with a crowding distance or neighbor density estimator to evaluate individuals. Pareto dominance-based algorithms work generally well to approximate PF in two or three objectives. However, the performance is severely deteriorated by the increasing number of objectives, because almost all the solutions are nondominated by each other under many objectives.

MOEA based on decomposition (MOEA/D) belongs to another scope to solve MOPs, which decomposes multiobjective problems into a number of scalar subproblems and optimizes them simultaneously. Classical MOEA/D mainly includes three decomposition approaches: weighted sum, weighted Tchebycheff [5] and boundary intersection [6]. A new penalty-based boundary intersection (PBI) approach is proposed in [7]. MOEA/D has several advantages over Pareto dominance-based algorithms such as computational efficiency, scalability to many problems and high search ability for combinatorial optimization problems. Despite its advantages, MOEA/D has two limitations: (1) MOEA/D is unable to produce an arbitrary number of weight vectors when the number of objectives is larger than two; (2) the weight vectors in classical MOEA/D are unchanged for different shapes of PF.

We propose a novel method called Pareto-adaptive weight vectors ($pa\lambda$), inspired by the Pareto-adaptive ϵ-dominance method that divides the objective space into different sizes of hyper boxes according to the geometrical characteristics of Pareto front [8]. The $pa\lambda$ approach has two important features: (1) $pa\lambda$ is based on Mixture Uniform Design (MUD) and able to generate an arbitrary number of weight vectors even when the number of objectives is larger than two; (2) $pa\lambda$ is driven by the hypervolume metric. It can automatically adjust weight vectors to scatter for concave PF, whereas assemble weight vectors for the convex PF. Experimental results on various multiobjective problems show that $pa\lambda$-MOEA/D obtains higher hypervolume, better convergence and more evenly distributed solutions than classical MOEA/D and NSGA-II.

II. $pa\lambda$: Pareto-adaptive Weight Vectors

The $pa\lambda$ is based on Mixture Uniform Design, and it automatically adjusts weight vectors by the shape of PF.

A. Weight Vectors by MUD

For MOEA/D, the number of weight vectors $N = C_{H+m-1}^{m-1}$ is controlled by the parameter H. When the number of objectives m is larger than 2, N is a discrete sequence for different H. $pa\lambda$ adopts *Mixture Uniform Design* (MUD) to produce an arbitrary number of evenly distributed weight vectors when $m \geq 3$.

MUD is an advanced experimental design method. Suppose that a vector is composed of m components $x_1, \cdots, x_m$. Each vector is one point in the space region $T^m = \{(x_1, \cdots, x_m) : x_i \geq 0; i = 1, \cdots, m; x_1 + \cdots + x_m = 1\}$. The opinion of MUD is to evenly spread the N experimental points (representing the N vectors) in region T^m. The detailed algorithm can be found in [9]. For example, in the case of $N = 10$ and $m = 3$, MUD first constructs an uniform design array $U_{10}(10^2)$, and then transfers U^{m-1} to C^{m-1} cubic space. The weight vectors $\lambda^k = (x_{k1}, x_{k2}, x_{k3})$, $k = 1, \cdots, N$ can be calculated as: $x_{k1} = 1 - \sqrt{c_{k1}}$, $x_{k2} = \sqrt{c_{k1}}(1 - c_{k2})$, and $x_{k3} = \sqrt{c_{k1}} c_{k2}$.

B. $pa\lambda$ for Two, Three and more Objectives

$pa\lambda$ controls weight vectors to assemble or scatter depending on the geometrical characteristics of PF. We first illustrate $pa\lambda$ in the bi-objective case. Assuming that PF is symmetric and the m objectives are normalized to $0 \leq f_i \leq 1$. The curve

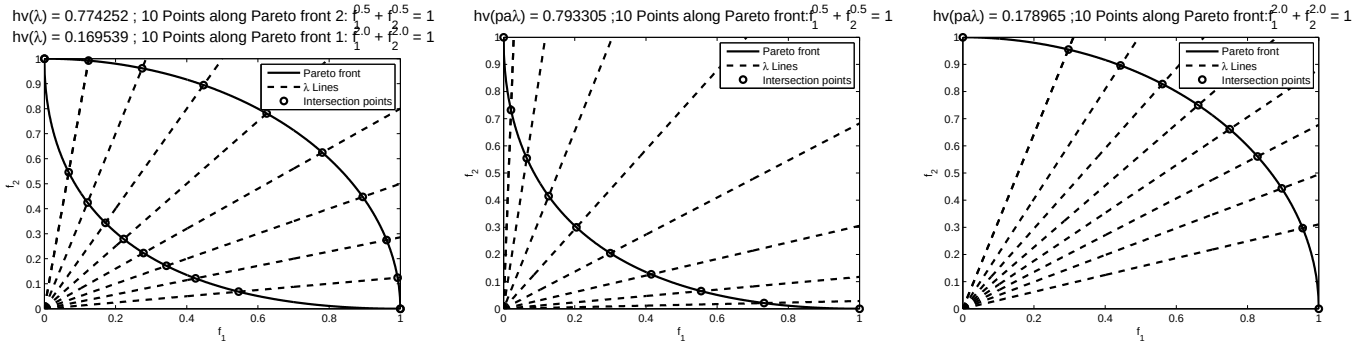

(a) λ (MOEA/D) for convex and concave PF (b) $pa\lambda$ for convex PF (c) $pa\lambda$ for concave PF

Fig. 1. 10 Intersection Points along 2-dimensional Pareto Front by λ (MOEA/D) and $pa\lambda$ Method

of PF can be represented as $f_1^p + f_2^p = 1$. The weight vectors satisfy $\lambda_1 + \lambda_2 = 1$, whose gradients are represented by λ lines (Figure 1). These λ lines produce N intersection points along PF. To evaluate the distribution of such points, we set the hypervolume metric [10] as a rule to drive $pa\lambda$ method.

When $p = 1$, the shape of PF is a line $f_1 + f_2 = 1$, the λ lines are distributed perfectly, and the set of intersection points has the maximum hypervolume. When $p \neq 1$, we need to move the intersection points until they are evenly distributed along $f_1^p + f_2^p = 1$. In other words, the intersection points with the maximum hypervolume is the ultimate goal. $pa\lambda$ introduces a *scale parameter* l to adjust the gradient of λ lines: $\frac{f_2}{f_1} = (\frac{\lambda_2}{\lambda_1})^l$. Define the intersection points as $\{(x_1^i, x_2^i), i = 1, \cdots, N\}$. They are along PF and on the adjusted λ lines: $(x_1^i)^p + (x_2^i)^p = 1; \frac{x_2^i}{x_1^i} = (\frac{\lambda_2^i}{\lambda_1^i})^l$.

For an assumptive scale parameter l, a set of intersection points is calculated by solving the above equations. Then, the hypervolume of such points is associated with the parameter l. $pa\lambda$ adopts Simplex Method to find evenly spread intersection points with the maximum hypervolume. The Simplex Method repeatedly uses the shrink, reflection and expansion procedures to get the optimal scale parameter l^{opt}. After that, the adjusted weight vectors can be calculated as:

$$\lambda_{pa\lambda}^i = (\frac{x_1^i}{x_1^i + x_2^i}, \frac{x_2^i}{x_1^i + x_2^i}) = \frac{(1, (\frac{\lambda_2^i}{\lambda_1^i})^{l^{opt}})}{1 + (\frac{\lambda_2^i}{\lambda_1^i})^{l^{opt}}}$$

Figure 1 shows an example of 10 intersection points along PF generated by λ (MOEA/D) and $pa\lambda$ respectively. When $p = 0.5$, the hypervolume of the intersection points is $hv = 0.774252$ by MOEA/D (plot (a) in Figure 1). From plot (b) in Figure 1, $pa\lambda$ gets the optimal parameter $l^{opt} = 1.7105$ and larger $hv = 0.793305$, the λ lines are scattered in the objective space, and the intersection points are moved to the two endpoints of PF. When $p = 2$, the hypervolume of intersection points is $hv = 0.169539$ by MOEA/D. $pa\lambda$ gets the optimal parameter $l^{opt} = 0.56192$ and larger $hv = 0.178965$ (plot (c) in Figure 1). λ lines are assembled together in the objective space, and the intersection points are moved to the median of PF.

For the tri-objectives case, $pa\lambda$ sets the number of *scale parameters* as 2. The λ lines are adjusted in two directions: in the plane xy the λ lines are adjusted by parameter l_2, and in the plane xz the λ lines are adjusted by parameter l_3. The intersection points along Pareto front and on the adjusted λ lines ($i = 1, \cdots, N$) can then be defined as:

$$(x_1^i)^p + (x_2^i)^p + (x_3^i)^p = 1; \quad \frac{x_2^i}{x_1^i} = (\frac{\lambda_2^i}{\lambda_1^i})^{l_2}; \quad \frac{x_3^i}{x_1^i} = (\frac{\lambda_3^i}{\lambda_1^i})^{l_3}$$

The two parameters l_2^{opt}, l_3^{opt} are optimized by the Simplex Method, and the adjusted weight vectors are calculated as:

$$\lambda_{pa\lambda}^i = \frac{(x_1^i, x_2^i, x_3^i)}{x_1^i + x_2^i + x_3^i} = \frac{(1, (\frac{\lambda_2^i}{\lambda_1^i})^{l_2^{opt}}, (\frac{\lambda_3^i}{\lambda_1^i})^{l_3^{opt}})}{1 + (\frac{\lambda_2^i}{\lambda_1^i})^{l_2^{opt}} + (\frac{\lambda_3^i}{\lambda_1^i})^{l_3^{opt}}}$$

$pa\lambda$ can expand to the case of more than three objectives. The scale parameters $(l_2, \cdots, l_m)$ are set for m objectives. At first, the weight vectors $\{\lambda^i = (\lambda_1^i, \cdots, \lambda_m^i) : i = 1, \cdots, N\}$ are initialized by MUD. Then, we estimate the p value of PF [8]. Finally, the scale parameters are optimized by the Simplex Method. The Pareto-adaptive weight vectors can then be calculated as follows: $r_j^i = (\lambda_j^i/\lambda_1^i)^{l_j^{opt}} (j = 2, \cdots, m)$ and $\lambda_{pa\lambda}^i = (1, r_2^i, \cdots, r_m^i)/(1 + \sum_{j=2}^m r_j^i)$.

III. The $pa\lambda$-MOEA/D Algorithm

The $pa\lambda$-MOEA/D algorithm is based on decomposition with Pareto-adaptive weight vectors, and its decomposition method is the Tchebycheff approach. A pseudo code of $pa\lambda$-MOEA/D is given in Algorithm 1. Some parameters are defined as: N is the size of population; T is the number of the neighborhood for weight vectors; $Archive$ is the external population which stores the non-dominated solutions.

There are four steps in the $pa\lambda$-MOEA/D: Step 1 is to initialize the first population, weight vectors, neighborhood and the external population ($Archive$); Step 2 is to generate the next offsprings, update population and $Archive$; Step 3 is the $pa\lambda$ method (as described in Section 2); and Step 4 is to quit the algorithm when the number of fitness function evaluations is larger than max_evals.

To explain, the initial weight vectors are generated by the *Mixture Uniform Design* (Line 5). As mentioned in Section II-A, by adopting MUD, we can generate an arbitrary number of weight vectors even when the number of objectives is larger than two. This expands the scalability of MOEA/D.

The $pa\lambda$ method is implemented as Lines 14-21. In Line 18, $pa\lambda$ estimates the parameter p of the Pareto-optimal front $f_1^p + \cdots + f_m^p = 1$ by calculating the area of non-dominated solutions in $Archive$ [8]. In Line 19, $pa\lambda$ is driven by the hypervolume metric (As described in section II-B). A larger hypervolume means that the intersection points distribute more evenly along the PF. $pa\lambda$ automatically adjusts the intersection points to scatter when PF is convex but assemble when PF is concave. There are $m-1$ parameters to be optimized for m objectives by the Simplex Method. In Lines 20-21, the new weight vectors are used to update the neighborhoods of each weight vector.

The algorithm finally outputs the non-dominated solutions in population when the stopping criteria is satisfied (Lines 23-25), which form the solutions of the multiobjective problem.

Algorithm 1: The $pa\lambda$-MOEA/D Method

1 **Step 1: Initialization Method**
2 Set $evals = 0, flag = false$;
3 Random generate first population X;
4 Evaluate X and update $evals$;
5 Generate first weight vectors λ by MUD;
6 Compute the T neighborhoods for every λ;
7 Add X into $Archive$ by dominance relationship;
8 **Step 2: Update Procedure**
9 **for** $i = 1, \cdots, N$ **do**
10 Generate a new solution y' from X by DE operator and polynomial mutation;
11 Evaluate y' and $evals++$;
12 Update population;
13 Add y' to $Archive$ by dominance relationship;
14 **Step 3: Pareto-adaptive λ Method**
15 **if** $flag == true$ *or* $|Archive| < 2N$ **then**
16 Go to **Step** 4;
17 Set $flag = true$;
18 Estimate parameter p of Pareto front for $Archive$;
19 Pareto-adaptive weight vectors;
20 Get the new weight vectors $\lambda = \lambda_{pa\lambda}$;
21 Recompute T neighborhoods for every λ;
22 **Step 4: Stopping Criteria**
23 **if** *evals* $< max\_evals$ **then**
24 Go to **Step 2**;
25 Output the non-dominated solutions in X.

IV. Experimental Results and Discussion

Experimental study to evaluate $pa\lambda$-MOEA/D against other competing approaches using jMetal 3.0, a Java-based framework that is aimed at facilitating the development of metaheuristics for solving MOPs, on benchmark problems.[1]

A. Test Problems and Experimental Setting

The test problems are ZDTx and DTLZx. ZDTx problem family include five bi-objective problems (ZDT1, ZDT2, ZDT3, ZDT4 and ZDT6). DTLZx problem family include seven tri-objective problems (DTLZ1, DTLZ2, DTLZ3, DTLZ4, DTLZ5, DTLZ6 and DTLZ7).

Five algorithms are tested including one Pareto dominance-based algorithm and four decomposition-based algorithms: NSGA-II, Non-Dominated Sorting Genetic Algorithm-II [2]; MOEA/D^{ws}, MOEA/D with the weight sum approach; MOEA/D^{te}, MOEA/D with the Tchebycheff approach [5]; MOEA/D^{pbi}, MOEA/D with the penalty-based boundary intersection approach [7]; and $pa\lambda$-MOEA/D, MOEA/D with Pareto-adaptive weight vectors.

The parameter settings are outlined as follows. The population size is 25 for ZDTx and 105 for DTLZx respectively. The number of weight vectors for the tri-objective problems in classical MOEA/D can be drew $C_{H+m-1}^{m-1} = C_{13+2}^{2} = 105$ when $H = 13$. The number of fitness function evaluations is $25,000$ for ZDTx and $50,000$ for DTLZx. Every algorithm launches 100 times independently for each test problem, to obtain statistically significant results. The number of neighborhoods T is 20. For DE (Differential Evolution) operator $CR = 1.0$ and $F = 0.5$. The probability of SBX crossover is 0.9. For polynomial mutation, $\eta = 20$ and $p_m = 1/n$, where n is the number of decisional variables.

We adopt five performance metrics: Hypervolume, Inverted Generational Distance (IGD), Generational Distance (GD), Unary Additive Epsilon Indicator ($I_{\epsilon+}^1$) and Spread. The higher Hypervolume and lower IGD, GD, $I_{\epsilon+}^1$ and Spread indicate the better performance. Results are compared using median values and the superior results of test problem are highlighted as grey background.

TABLE I
Median of Hypervolume (**HV**)

	MOEA/D^{ws}	MOEA/D^{te}	MOEA/D^{pbi}	NSGA-II	$pa\lambda$-MOEA/D
ZDT1	$6.521e-01$	$6.392e-01$	$6.057e-01$	$6.381e-01$	$6.412e-01$
ZDT2	$0.000e+00$	$3.097e-01$	$2.957e-01$	$3.060e-01$	$3.107e-01$
ZDT3	$4.863e-01$	$4.870e-01$	$4.642e-01$	$5.066e-01$	$4.873e-01$
ZDT4	$3.534e-01$	$6.360e-01$	$6.244e-01$	$6.359e-01$	$6.391e-01$
ZDT6	$0.000e+00$	$3.857e-01$	$3.857e-01$	$3.709e-01$	$3.859e-01$
DTLZ1	$2.259e-01$	$7.434e-01$	$7.835e-01$	$7.262e-01$	$7.814e-01$
DTLZ2	$0.000e+00$	$3.777e-01$	$3.812e-01$	$3.766e-01$	$4.074e-01$
DTLZ3	$0.000e+00$	$3.605e-01$	$2.633e-01$	$1.901e-01$	$3.817e-01$
DTLZ4	$0.000e+00$	$3.774e-01$	$3.583e-01$	$3.759e-01$	$3.962e-01$
DTLZ5	$0.000e+00$	$8.936e-02$	$7.789e-02$	$9.296e-02$	$9.156e-02$
DTLZ6	$0.000e+00$	$9.035e-02$	$7.786e-02$	$4.259e-03$	$9.266e-02$
DTLZ7	$2.673e-02$	$1.944e-01$	$2.151e-01$	$2.808e-01$	$2.471e-01$

[1] http://jmetal.sourceforge.net [11]

B. Statistical Results of Performance Metrics

Table I summarizes the performance for the hypervolume measure, which evaluates both convergence and distribution of non-dominated solutions. Among the 12 test problems, $pa\lambda$-MOEA/D obtains the best results on 7 problems. MOEA/D^{ws} obtains zero hypervolume for ZDT2, ZDT6 (PF: $f_1^2 + f_2 = 1$) and DTLZ2-6 (PF: $f_1^2 + f_2^2 + f_3^2 = 1$). The result indicates that weighted sum approach is not suitable for dealing with concave PF.

Both MOEA/D^{te} and $pa\lambda$-MOEA/D use Tchebycheff approach, $pa\lambda$-MOEA/D obtains higher hypervolume than MOEA/D^{te} on all the 12 problems. Comparing the dominance-based and decomposition-based algorithms, NSGA-II outperforms MOEA/D on ZDT3, DTLZ5 and DTLZ7. Future analysis on the shape of ZDT3 and DTLZ7, they are formed to be discrete PF , respectively. This indicates that decomposition methods are generally less suitable for dealing with problems with discrete PF.

TABLE II
MEDIAN OF INVERTED GENETIC DISTANCE (**IGD**)

	MOEA/D^{ws}	MOEA/D^{te}	MOEA/D^{pbi}	NSGA-II	$pa\lambda$-MOEA/D
ZDT1	$5.421e-04$	$6.484e-04$	$1.143e-03$	$7.943e-04$	$5.797e-04$
ZDT2	$1.302e-02$	$5.844e-04$	$7.028e-04$	$8.155e-04$	$6.022e-04$
ZDT3	$4.934e-03$	$2.012e-03$	$2.062e-03$	$1.197e-03$	$1.973e-03$
ZDT4	$7.017e-03$	$6.654e-04$	$7.854e-04$	$8.141e-04$	$5.938e-04$
ZDT6	$6.763e-03$	$3.697e-04$	$3.704e-04$	$7.327e-04$	$4.131e-04$
DTLZ1	$4.034e-03$	$6.928e-04$	$4.212e-04$	$7.907e-04$	$4.520e-04$
DTLZ2	$5.346e-03$	$7.422e-04$	$6.148e-04$	$7.584e-04$	$5.779e-04$
DTLZ3	$1.419e-02$	$1.237e-03$	$1.897e-03$	$3.587e-03$	$1.179e-03$
DTLZ4	$5.876e-03$	$1.160e-03$	$7.430e-04$	$1.199e-03$	$7.215e-04$
DTLZ5	$1.382e-03$	$5.222e-05$	$1.106e-04$	$1.891e-05$	$2.789e-05$
DTLZ6	$3.291e-03$	$1.264e-04$	$2.789e-04$	$1.717e-03$	$6.776e-05$
DTLZ7	$1.245e-02$	$5.590e-03$	$4.031e-03$	$2.181e-03$	$3.555e-03$

Table II shows the performance for the Inverted Genetic Distance metric, which also evaluates both convergence and distribution of non-dominated solutions. For 12 test problems, $pa\lambda$-MOEA/D obtains the best results on more problems than any other methods do. Comparing MOEA/D and NSGA-II except for the discrete PF (ZDT3 and DTLZ7), MOEA/D^{pbi} outperform NSGA-II on 8 problems (except ZDT1 and DTLZ5), which is similar to the results reported in [7]. For the same Tchebycheff approach, $pa\lambda$-MOEA/D outperform MOEA/D^{te} on 10 problems except ZDT2 and ZDT6.

TABLE III
MEDIAN OF GENETIC DISTANCE (**GD**)

	MOEA/D^{ws}	MOEA/D^{te}	MOEA/D^{pbi}	NSGA-II	$pa\lambda$-MOEA/D
ZDT1	$4.411e-02$	$9.595e-04$	$6.162e-03$	$1.007e-03$	$9.155e-04$
ZDT2	$4.400e-02$	$5.806e-04$	$2.727e-03$	$1.182e-03$	$6.249e-04$
ZDT3	$2.374e-02$	$1.732e-03$	$8.772e-03$	$5.412e-04$	$1.801e-03$
ZDT4	$1.760e+00$	$1.536e-03$	$3.422e-03$	$7.354e-04$	$1.296e-03$
ZDT6	$2.632e-02$	$9.647e-04$	$9.568e-04$	$9.654e-04$	$1.242e-03$
DTLZ1	$2.874e+01$	$1.137e-03$	$1.123e-03$	$2.406e-02$	$8.056e-04$
DTLZ2	$5.362e-02$	$9.088e-04$	$2.585e-03$	$1.342e-03$	$7.247e-04$
DTLZ3	$3.115e+01$	$1.977e-03$	$1.114e-02$	$6.101e-02$	$1.666e-03$
DTLZ4	$5.262e-02$	$7.847e-03$	$6.524e-03$	$4.943e-03$	$5.726e-03$
DTLZ5	$1.773e-02$	$2.990e-04$	$9.180e-02$	$3.625e-04$	$2.761e-04$
DTLZ6	$1.153e-01$	$6.546e-04$	$9.217e-02$	$3.321e-02$	$5.264e-04$
DTLZ7	$1.433e-01$	$1.663e-03$	$4.780e-03$	$2.741e-03$	$1.566e-03$

Tables III and IV show the performance for the Genetic Distance and epsilon metrics respectively. Among the 12 test problems, $pa\lambda$-MOEA/D obtains the best results of these two metrics on most of the problems.

TABLE IV
MEDIAN OF **EPSILON** ($I^1_{\epsilon+}$) METRIC

	MOEA/D^{ws}	MOEA/D^{te}	MOEA/D^{pbi}	NSGA-II	$pa\lambda$-MOEA/D
ZDT1	$2.964e-02$	$3.381e-02$	$4.810e-02$	$4.457e-02$	$2.524e-02$
ZDT2	$3.819e-01$	$2.767e-02$	$3.831e-02$	$4.497e-02$	$3.200e-02$
ZDT3	$6.133e-02$	$6.034e-02$	$9.272e-02$	$2.996e-02$	$5.514e-02$
ZDT4	$3.126e-01$	$3.438e-02$	$3.879e-02$	$4.749e-02$	$2.658e-02$
ZDT6	$3.470e-01$	$1.931e-02$	$1.932e-02$	$4.058e-02$	$1.901e-02$
DTLZ1	$2.721e-01$	$4.752e-02$	$3.050e-02$	$7.337e-02$	$3.546e-02$
DTLZ2	$4.215e-01$	$1.004e-01$	$9.093e-02$	$1.214e-01$	$8.279e-02$
DTLZ3	$1.009e+00$	$1.156e-01$	$1.698e-01$	$2.788e-01$	$1.067e-01$
DTLZ4	$4.060e-01$	$9.668e-02$	$9.978e-02$	$1.068e-01$	$9.303e-02$
DTLZ5	$2.437e-01$	$1.887e-02$	$4.289e-02$	$1.016e-02$	$1.454e-02$
DTLZ6	$2.437e-01$	$1.863e-02$	$4.242e-02$	$2.223e-01$	$1.427e-02$
DTLZ7	$7.474e-01$	$2.605e-01$	$2.396e-01$	$1.269e-01$	$1.849e-01$

Table V shows the performance for the Spread metric, which evaluates distribution of non-dominated solutions. $pa\lambda$-MOEA/D obtains the best results on 8 problems. NSGA-II gets 3 best results on ZDT3, DTLZ5 and DTLZ7. For the bi-objective problems by MOEA/D, $pa\lambda$-MOEA/D brings about a larger spread value improvement when PF is convex (ZDT1, ZDT4), but smaller when PF is concave (ZDT6). The poor performance on ZDT3 for $pa\lambda$-MOEA/D may attribute that $pa\lambda$ cannot estimate well the parameter p for discrete PF. For the tri-objective problems by MOEA/D, $pa\lambda$-MOEA/D improves the spread values on almost all problems.

TABLE V
MEDIAN OF **SPREAD** METRIC

	MOEA/D^{ws}	MOEA/D^{te}	MOEA/D^{pbi}	NSGA-II	$pa\lambda$-MOEA/D
ZDT1	$1.299e+00$	$2.841e-01$	$2.433e-01$	$4.093e-01$	$1.423e-01$
ZDT2	$1.960e+00$	$1.427e-01$	$1.559e-01$	$4.253e-01$	$1.251e-01$
ZDT3	$1.800e+00$	$7.760e-01$	$5.816e-01$	$5.432e-01$	$8.184e-01$
ZDT4	$1.945e+00$	$2.912e-01$	$2.538e-01$	$4.812e-01$	$1.462e-01$
ZDT6	$1.939e+00$	$1.496e-01$	$1.494e-01$	$7.566e-01$	$1.462e-01$
DTLZ1	$1.440e+00$	$8.717e-01$	$6.221e-01$	$8.434e-01$	$5.592e-01$
DTLZ2	$1.642e+00$	$9.028e-01$	$6.470e-01$	$6.982e-01$	$5.495e-01$
DTLZ3	$1.573e+00$	$9.199e-01$	$6.420e-01$	$8.352e-01$	$7.196e-01$
DTLZ4	$1.572e+00$	$9.223e-01$	$6.705e-01$	$6.661e-01$	$6.443e-01$
DTLZ5	$1.633e+00$	$1.138e+00$	$1.050e+00$	$4.418e-01$	$6.993e-01$
DTLZ6	$1.513e+00$	$1.153e+00$	$1.193e+00$	$8.233e-01$	$6.915e-01$
DTLZ7	$1.493e+00$	$1.111e+00$	$9.475e-01$	$7.453e-01$	$9.711e-01$

In conclusion, the results in Tables 1-5 confirm that $pa\lambda$-MOEA/D is able to obtain consistently higher hypervolume, better convergence and more evenly distributed solutions than classical MOEA/D and NSGA-II on most of the benchmark problems considered. The core feature of $pa\lambda$ views the elasticity of the weight vectors that adapts according to the geometrical characteristics of PF. In addition, $pa\lambda$-MOEA/D largely dominates other MOEA/D methods especially for solving tri-objective problems.

C. $pa\lambda$ with Arbitrary Number of Weight Vectors

The number of weight vectors in classical MOEA/D is set to be $N = C^{m-1}_{H+m-1}$. For tri-objective problems, $N = \{45, 55, ..., 91, 105, 120, 136, 153, 171, 190, 210, 231, 253\}$, which is discrete for $H = \{8, 9, \cdots, 25\}$. $pa\lambda$-MOEA/D, on the other hand, is not constrain to specific size, and able to generate an arbitrary number of weight vectors when the number of objectives is larger than 2 (Section II-A).

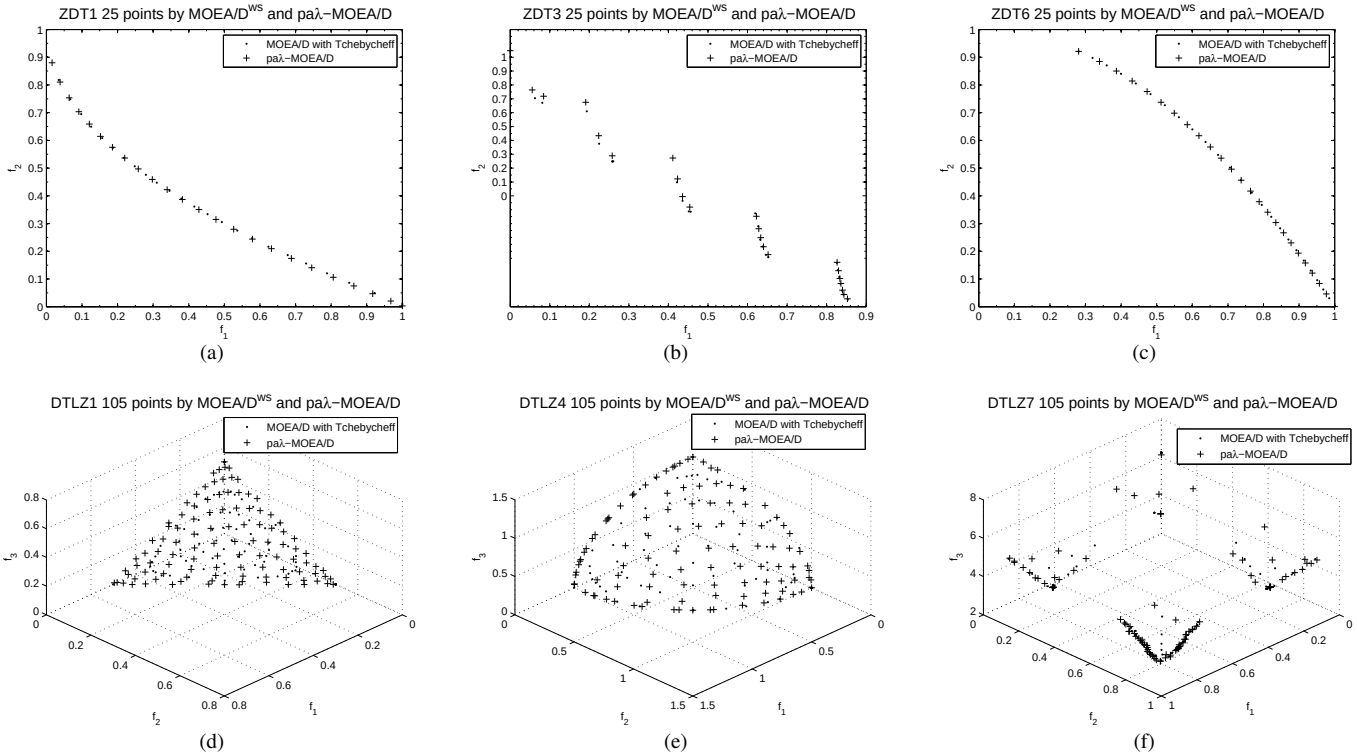

Fig. 2. The Efficient Pareto-optimal Solutions Obtained by MOEA/D^{te} and $pa\lambda$-MOEA/D

In Table VI, we compare $pa\lambda$-MOEA/D with NSGA-II on tri-objective problem DTLZ2. The population size is set as $N = 50, 100, 150, 200, 250$. The maximum evaluation times is 50000. Table VI exhibits that $pa\lambda$-MOEA/D gets higher hypervolume than NSGA-II for different population sizes. The statistical results thus indicate that $pa\lambda$-MOEA/D is not only able to generate an arbitrary number of weight vectors, but also more efficient than NSGA-II.

TABLE VI
MEDIAN OF **HV** FOR ARBITRARY NUM OF WEIGHT VECTORS

	N = 50	N = 100	N =150	N = 200	N = 250
NSGA-II	$3.383e-1$	$3.728e-1$	$3.914e-1$	$4.037e-1$	$4.110e-1$
$pa\lambda$-MOEA/D	$3.773e-1$	$4.058e-1$	$4.107e-1$	$4.268e-1$	$4.315e-1$

V. CONCLUSION AND FUTURE RESEARCH

In this paper, we propose the novel $pa\lambda$-MOEA/D algorithm. It automatically adjusts the weight vectors based on the geometrical characteristics of PF. Experiments on 12 benchmark problems confirm that it outperforms classical MOEA/D and NSGA-II in term of the hypervolume, Inverted Genetic Distance, Genetic Distance, epsilon and Spread metrics.

$pa\lambda$-MOEA/D assumes that PF is symmetric. For an asymmetric curve $f_1^{p_1} + f_2^{p_2} = 1$ ($p_1 \neq p_2$), classical MOEA/D are not suitable to deal with such asymmetric MOPs. The future research will focus on the challenging problem of automatically adjusting weight vectors for asymmetric PF. Another interesting issue is to adopt Memetic Computation to optimize the MOPs [12], [13], [14].

REFERENCES

[1] C. Coello, "Evolutionary multi-objective optimization: A historical view of the field," *IEEE Compu. Intell. Magazine*, 2006.

[2] K. Deb, A. Pratap, S. Agarwal, and T. Meyarivan, "A fast and elitist multiobjective genetic algorithm: NSGA-II," *IEEE Trans. Evol. Comput.*, 2002.

[3] E. Zitzler, M. Laumanns, and L. Thiele, "Spea2: Improving the strength pareto evolutionary algorithm," *Technical Report 103, Computer Engineering and Networks Laboratory*, 2001.

[4] A. Nebro, J. Durillo, J. Garcá-Nieto, C. Coello, F. Luna, and E. Alba, "Smpso: A new pso-based metaheuristic for multi-objective optimization," in *IEEE Symp. on MCDM*, 2009.

[5] K. Miettinen, *Nonlinear multiobjective optimization*. Springer, 1999.

[6] I. Das and J. E. Dennis, "Normal-bounday intersection: A new method for generating pareto optimal points in multicriteria optimization problems," *SIAM Journal of Optimization*, 1998.

[7] H. Li and Q. Zhang, "Multiobjective optimization problems with complicated Pareto sets, MOEA/D and NSGA-II," *IEEE Trans. Evol. Comput.*, 2009.

[8] A. G. Hernández-Díaz, L. V. Santana-Quintero, C. A. C. Coello, and J. Molina, "Pareto-adaptive epsilon-dominance," *Evol. Comput.*, 2007.

[9] K. Fang and C. Ma, *Orthogonal and uniform design*. Science Press, 2001.

[10] E. Zitzler and L. Thiele, "Multiobjective evolutionary algorithms: A comparative case study and the strength pareto approach," *IEEE Trans. Evol. Comput.*, 2002.

[11] J. Durillo, A. Nebro, and E. Alba, "The jmetal framework for multi-objective optimization: Design and architecture," *Proceedings of the IEEE Congr. Evol. Comput.*, 2010.

[12] D. Lim, Y. Jin, Y. Ong, and B. Sendhoff, "Generalizing surrogate-assisted evolutionary computation," *IEEE Trans. Evol. Comput.*, 2010.

[13] Y. Ong, M. Lim, N. Zhu, and K. Wong, "Classification of adaptive memetic algorithms: A comparative study," *IEEE Trans. on Systems, Man, and Cybernetics, Part B: Cybernetics*, 2006.

[14] Y. Ong, M. Lim, and X. Chen, "Research frontier: memetic computation-past, present & future," *IEEE Comput. Intell. Mag*, 2010.